Commun. Comput. Phys.
doi: 10.4208/cicp.OA-2016-0261

Vol. **22**, No. 4, pp. 889-912
October 2017

An Implicit Unified Gas Kinetic Scheme for Radiative Transfer with Equilibrium and Non-Equilibrium Diffusive Limits

Wenjun Sun[1], Song Jiang[1] and Kun Xu[2,*]

[1] *Institute of Applied Physics and Computational Mathematics, Fenghao East Road 2, Haidian District, Beijing 100094, China.*
[2] *Department of Mathematics, Hong Kong University of Science and Technology, Hong Kong.*

Received 19 December 2016; Accepted (in revised version) 28 March 2017

Abstract. This paper is about the construction of a unified gas-kinetic scheme (UGKS) for a coupled system of radiative transport and material heat conduction with different diffusive limits. Different from the previous approach, instead of including absorption/emission only, the current method takes both scattering and absorption/emission mechanism into account in the radiative transport process. As a result, two asymptotic limiting solutions will appear in the diffusive regime. In the strong absorption/emission case, an equilibrium diffusion limit is obtained, where the system is mainly driven by a nonlinear diffusion equation for the equilibrium radiation and material temperature. However, in the strong scattering case, a non-equilibrium limit can be obtained, where coupled nonlinear diffusion system with different radiation and material temperature is obtained. In addition to including the scattering term in the transport equation, an implicit UGKS (IUGKS) will be developed in this paper as well. In the IUGKS, the numerical flux for the radiation intensity is constructed implicitly. Therefore, the conventional CFL constraint for the time step is released. With the use of a large time step for the radiative transport, it becomes possible to couple the IUGKS with the gas dynamic equations to develop an efficient numerical method for radiative hydrodynamics. The IUGKS is a valid method for all radiative transfer regimes. A few numerical examples will be presented to validate the current implicit method for both optical thin to optical thick cases.

PACS: 44.40.+a, 45.10.-b, 05.60.Cd, 02.60.Cb

Key words: Radiative transfer, asymptotic preserving, implicit method, multiscale modeling.

*Corresponding author. *Email addresses:* sun_wenjun@iapcm.ac.cn (W. Sun), jiang@iapcm.ac.cn (S. Jiang), makxu@ust.hk (K. Xu)

 ©2017 Global-Science Press

https://doi.org/10.4208/cicp.OA-2016-0261 Published online by Cambridge University Press

1 Introduction

This paper is about the construction of unified gas kinetic scheme (UGKS) for a system with coupled radiative transfer and material temperature evolution equations. For the radiative transport part, besides capturing absorption/emission mechanism in the previous UGKS method, the scattering process is taken into account as well in this paper. As a coupled system, for the low opacity material, such as the case with small absorption/emission coefficient and small scattering coefficient, the interaction between the radiation and material is weak, and the radiation propagates in a transparent way with particle-type behavior, the so-called optical thin regime. In this regime, the numerical method for radiation is basically to solve the streaming transport equation with upwind approach, such as ray tracking in SN methods. For a high opacity material, which has large absorption/emission coefficient or large scattering coefficient, the severe energy exchange between the radiation and material heat evolution makes photon's mean free path diminish. As a result, different asymptotic limits in the optical thick regime will appear. In the case with large absorption/emission coefficients, an equilibrium diffusive process for radiation will emerge and the material temperature and the radiation temperature will get the same value. The previous UGKS solves the equations with the absorption/emission only and captures the above diffusive limit [14, 15]. However, for the case with highly scattering material, the diffusive limiting equation will still include different temperatures for the radiation and material, with a coupled temperature evolution equation in the so-called non-equilibrium diffusive regime [19, 20]. In this paper, the previous UGKS will be extended to capture such a non-equilibrium diffusive regime. More importantly, besides recovering different limiting regimes, the aim of UGKS is to present accurate solutions in all regimes efficiently from the transparent to the diffusive evolutions. Different regimes in UGKS are identified automatically through the the ratio of the local cell size to the local photon's mean free path, with a smooth transition across all transport regimes. The UGKS framework was developed in [12]. The previous UGKS studies for radiative transfer include the linear radiation transport model [10], or the gray and frequency-dependent radiative transfer systems [14, 15]. The critical step in UGKS is to construct a time evolving solution for the radiation intensity at a cell interface for the flux evaluation. Depending on the ratio of the time cell size to the photon's mean free path, the evolution solution covers all regimes from the kinetic scale free transport to the hydrodynamic diffusive evolution. As a result, the cell size and time step in UGKS are not limited by the photon's mean free path and collision time [1, 3]. The efficiency of the UGKS in different regimes is achieved by solving the coupled macroscopic evolution equations for the radiation energy and material thermal energy first, before updating the source terms in the discretized radiative transport equation.

In the previous UGKS for radiative transfer, the numerical time step is controlled by the CFL condition, which is determined by the ratio of the cell size over the speed of light. In order to couple the radiative transfer equation with hydrodynamic equations, this small time step restriction for radiation will constrain severely the computational ef-

https://doi.org/10.4208/cicp.OA-2016-0261 Published online by Cambridge University Press

ficiency for the radiation-hydrodynamic system. In order to overcome this kind of time step barrier in the UGKS, an implicit unified gas kinetic scheme (IUGKS) will be developed in this paper for the radiative transfer system as well. For the IUGKS, the CFL condition is released and a large time step can be used.

This paper is organized as follows. Section 2 presents the model equations of gray radiation transfer with the inclusion of scattering and absorption/emission. Section 3 is about the construction of IUGKS for the system. Section 4 presents the asymptotic preserving property of IUGKS. In Section 5 the IUGKS is extended to solve the frequency-dependent radiative transfer system. Section 6 includes a number of numerical tests to validate the accuracy and robustness of the proposed scheme. A conclusion is given in the last section.

2 Radiative transfer system with scattering and absorption/emission

The gray radiative transfer system describes the radiative transfer and the energy exchange between radiation and materials. The system with strong isotropic scattering can be written in following scaled form:

$$\begin{cases} \dfrac{\epsilon}{c}\dfrac{\partial I}{\partial t}+\vec{\Omega}\cdot\nabla I=\mathcal{L}_a^\epsilon\sigma_a\Big(\dfrac{1}{4\pi}acT^4-I\Big)+\mathcal{L}_s^\epsilon\sigma_s\Big(\dfrac{1}{4\pi}\displaystyle\int_{4\pi}Id\Omega-I\Big), \\ C_v\dfrac{\partial T}{\partial t}\equiv\dfrac{\partial U}{\partial t}=\dfrac{\mathcal{L}_a^\epsilon\sigma_a}{\epsilon}\Big(\displaystyle\int Id\vec{\Omega}-acT^4\Big)+\nabla\cdot(\chi\nabla T). \end{cases} \tag{2.1}$$

Here the spatial variable is denoted by $\vec{r}$, $\vec{\Omega}$ is the angular variable, and t is the time variable, $I(\vec{r},\vec{\Omega},t)$ is the radiation intensity, $T(\vec{r},t)$ is the material temperature, $\sigma_a(\vec{r},T)$ is the absorption coefficient, $\sigma_s(\vec{r},T)$ is the scattering coefficient, a is the radiation constant, c is the speed of light, $\epsilon>0$ is the Knudsen number, $\mathcal{L}_a^\epsilon$ and $\mathcal{L}_s^\epsilon$ are two parameters depending on ϵ, $U(\vec{r},t)$ is the material energy density, and χ is the conductivity of the material. In this paper, $\phi=acT^4$ is defined. For the simplicity of presentation, we have omitted the internal source in (2.1). According to Spitzer and Harm [13], the material conduction coefficient χ for the electron thermal conductivity in a fully ionized gas has the following form,

$$\chi=1.0*10^{-2}T^{5/2}.$$

For system (2.1), both scattering and absorption will take effect. Depending on the values of $\mathcal{L}_a^\epsilon$ and $\mathcal{L}_s^\epsilon$, which are functions of ϵ, the system can relax to different equilibrium states in the diffusive regime. With $\mathcal{L}_a^\epsilon=1/\epsilon$ and $\mathcal{L}_s^\epsilon=\epsilon$, as $\epsilon\to0$ the equilibrium state with equal radiation and material temperature and Planckian distribution will be obtained,

$$I\longrightarrow\frac{acT_0^4}{4\pi},$$

https://doi.org/10.4208/cicp.OA-2016-0261 Published online by Cambridge University Press

and the material temperature T_0 satisfies the following evolution equation,

$$\frac{\partial}{\partial t}U(T^{(0)})+a\frac{\partial}{\partial t}(T^{(0)})^4=\nabla\cdot\frac{ac}{3\sigma_a}\nabla(T^{(0)})^4. \tag{2.2}$$

With $\mathcal{L}_a^\epsilon=\epsilon$ and $\mathcal{L}_s^\epsilon=1/\epsilon$, as $\epsilon\to 0$ the non-equilibrium states will be approached. With the definition of radiation energy $\rho=\int Id\Omega$, in this limit the intensity I goes to

$$I^{(0)}=\frac{\rho}{4\pi},$$

and the radiation energy and material temperature T satisfy the following nonlinear non-equilibrium diffusion equations,

$$\begin{cases}\dfrac{\partial\rho}{\partial t}-\nabla\cdot\dfrac{c}{3\sigma_s}\nabla\rho=c\sigma_a(acT^4-\rho),\\ C_v\dfrac{\partial T}{\partial t}\equiv\dfrac{\partial U}{\partial t}=\sigma_a\Big(\rho-acT^4\Big)+\nabla\cdot(\chi\nabla T).\end{cases} \tag{2.3}$$

An asymptotic preserving (AP) scheme for the gray radiation transfer system (2.1) should lead to the correct discretization of the equilibrium diffusion equation (2.2) in the strong absorption/emission case, and to the non-equilibrium diffusion limit (2.3) in the strong scattering case. At the same time, the AP scheme should be uniformly stable in ϵ. The IUGKS in this paper for (2.1) captures the limiting equations (2.2) or (2.3) automatically at small ϵ case, and it provides accurate solution in all other regimes.

3 An implicit unified gas kinetic scheme for radiative transfer system

In this section, we will extend the UGKS in [14,15] for both gray and frequency-dependent radiative system to the system with strong isotropic scattering as well. At the same time, an implicit unified gas kinetic scheme (IUGKS) for (2.1) will be constructed.

3.1 Angular, spatial, and time discretization

The discrete ordinate method (DOM) is used to solve the radiative transfer equations (2.1). Here only the two-dimensional case with Cartesian coordinates is considered. In this case, the angle direction $\vec{\Omega}=(\mu,\xi)$ has components $\mu=\sqrt{1-\zeta^2}\cos\theta$ and $\xi=\sqrt{1-\zeta^2}\sin\theta$, where $\zeta\in[-1,1]$ is the cosine value of the angle between the propagation direction $\vec{\Omega}$ and the z-axis, and $\theta\in[0,2\pi)$ is the angle between the projection vector of $\vec{\Omega}$ onto the xy-plane and the x-axis. Due to the symmetry of angular distribution in the two-dimensional Cartesian case, we only need to consider $\zeta\geq 0$.

For the angular variable of the equation (2.1), as done in DOM, the propagation direction $\vec{\Omega}=(\mu,\xi)$ is discretized with discrete directions. One standard method is to use

https://doi.org/10.4208/cicp.OA-2016-0261 Published online by Cambridge University Press

a symmetric quadrature set with N discrete ξ values, each ξ value having M_n number of discrete μ values. Other quadrature sets can be used as well. As presented in [9], an even integer N is used for discrete directions (μ_m,ξ_m) with the total number $m=1,\cdots,M$ with $M=N(N+2)/2$ and the corresponding integration weight ω_m. In each direction (μ_m,ξ_m), we have the following discrete equation,

$$\begin{cases} \dfrac{\epsilon}{c}\partial_t I_m+(\mu_m\partial_x I_m+\xi_m\partial_y I_m)=\mathcal{L}_a^\epsilon\sigma_a\Big(\dfrac{1}{2\pi}\phi-I_m\Big)+\mathcal{L}_s^\epsilon\sigma_s\Big(\dfrac{\rho}{2\pi}-I_m\Big), \\ C_v\partial_t T=\dfrac{\mathcal{L}_a^\epsilon\sigma_a}{\epsilon}\Big(\sum\limits_{i=1}^{M}\omega_i I_i-\phi\Big)+\nabla\cdot(\chi\nabla T), \qquad m=1,\cdots,M. \end{cases} \tag{3.1}$$

For the spatial and time variables, let $x_i=i\Delta x$, $y_j=j\Delta y$, and $t^n=n\Delta t$ $(i,j,n\in\mathbb{Z})$ be the uniform meshes in Cartesian coordinates, where $\Delta x,\Delta y$, and Δt are the mesh sizes in the x-, y- and t-directions, respectively. Let (i,j) denote the cell $\{(x,y);\, x_{i-1/2}<x<x_{i+1/2},y_{j-1/2}<y<y_{j+1/2}\}$, where $x_{i-1/2}=(i-\frac{1}{2})\Delta x$ and $y_{j-1/2}=(j-\frac{1}{2})\Delta y$ are the cell interfaces.

The finite volume method will be used to discretize the above equations (3.1). So in the following, we use $I_{i,j,m}^n$ to denote the cell averaged value for variable I_m at time t^n in cell (i,j) with cell center $(x_{i,j},y_{i,j})$. When integrating equation (3.1) over the cell (i,j) from time t^n to $t^n+\Delta t$, a conservative finite volume numerical scheme for equation (3.1) is of the form

$$\begin{cases} I_{i,j,m}^{n+1}=I_{i,j,m}^n+\dfrac{\Delta t}{\Delta x}(F_{i-1/2,j,m}-F_{i+1/2,j,m})+\dfrac{\Delta t}{\Delta y}(H_{i,j-1/2,m}-H_{i,j+1/2,m}) \\ \qquad\qquad +c\Delta t\Big\{\dfrac{\mathcal{L}_a^\epsilon\sigma_a}{\epsilon}\Big(\dfrac{1}{2\pi}\tilde{\phi}_{i,j}-\tilde{I}_{i,j,m}\Big)\Big\}+c\Delta t\Big\{\dfrac{\mathcal{L}_s^\epsilon\sigma_s}{\epsilon}\Big(\dfrac{1}{2\pi}\tilde{\rho}_{i,j}-\tilde{I}_{i,j,m}\Big)\Big\}, \\ C_v\dfrac{T_{i,j}^{n+1}-T_{i,j}^n}{\Delta t}=\dfrac{\mathcal{L}_a^\epsilon\sigma_a}{\epsilon}\Big(\sum\limits_{m=1}^{M}\omega_m\tilde{I}_{i,j,m}-\tilde{\phi}_{i,j}\Big)+\dfrac{1}{\Delta x}(M_{i+1/2,j}-M_{i-1/2,j}) \\ \qquad\qquad +\dfrac{1}{\Delta y}(M_{i,j+1/2}-M_{i,j-1/2}), \end{cases} \tag{3.2}$$

where $F_{i-1/2,j,m}$ and $H_{i,j-1/2,m}$ are the time-dependent numerical fluxes in the x- and y-direction across the cell interface for the radiative transfer, and $M_{i\pm1/2,j}$ and $M_{i,j\pm1/2}$ are the time-dependent diffusive fluxes for in material temperature evolution. The explicit expressions for the terms on the right hand side of (3.2) are given by

$$F_{i-1/2,j,m}=\frac{c}{\epsilon\Delta t}\int_{t^n}^{t^{n+1}}\mu_m I_m(t,x_{i-\frac{1}{2}},y_j,\mu_m,\xi_m)dt, \tag{3.3a}$$

$$H_{i,j-1/2,m}=\frac{c}{\epsilon\Delta t}\int_{t^n}^{t^{n+1}}\xi_m I_m(t,x_i,y_{j-\frac{1}{2}},\mu_m,\xi_m)dt, \tag{3.3b}$$

$$M_{i-1/2,j}=\frac{1}{\Delta t}\int_{t^n}^{t^{n+1}}\Big(\chi\frac{\partial T}{\partial x}\Big)(t,x_{i-\frac{1}{2}},y_j)dt, \tag{3.3c}$$

https://doi.org/10.4208/cicp.OA-2016-0261 Published online by Cambridge University Press

$$M_{i,j-1/2}=\frac{1}{\Delta t}\int_{t^n}^{t^{n+1}}\left(\chi\frac{\partial T}{\partial y}\right)(t,x_i,y_{j-\frac{1}{2}})dt, \tag{3.3d}$$

$$\tilde{\phi}_{i,j}=\frac{1}{2\pi\Delta t\Delta x\Delta y}\int_{t^n}^{t^{n+1}}\int_{x_{i-1/2}}^{x_{i+1/2}}\int_{y_{j-1/2}}^{y_{j+1/2}}\phi(t,x,y)dxdydt, \tag{3.3e}$$

$$\tilde{\rho}_{i,j}=\frac{1}{2\pi\Delta t\Delta x\Delta y}\int_{t^n}^{t^{n+1}}\int_{x_{i-1/2}}^{x_{i+1/2}}\int_{y_{j-1/2}}^{y_{j+1/2}}\rho(t,x,y)dxdydt, \tag{3.3f}$$

$$\tilde{I}_{i,j,m}=\frac{1}{\Delta x\Delta y\Delta t}\int_{t^n}^{t^{n+1}}\int_{x_{i-1/2}}^{x_{i+1/2}}\int_{y_{j-1/2}}^{y_{j+1/2}}I_m(t,x,y,\mu_m,\xi_m)dxdydt. \tag{3.3g}$$

In order to update system (3.2), we have to determine all terms in (3.3). First, for an implicit scheme the term $\tilde{I}_{i,j,m}$ in (3.3) can be approximated implicitly as

$$\tilde{I}_{i,j,m}\approx I^{n+1}_{i,j,m},$$

which can be combined with the solution on the left hand side of Eq. (3.2).

For spatial discretization $M_{i-1/2,j}$ term in (3.3), the conservative approach in [16] is used

$$M_{i-1/2,j}=\chi_{i-1/2,j}\frac{T^{n+1}_{i,j}-T^{n+1}_{i-1,j}}{\Delta x},$$

where

$$\chi_{i-1/2,j}=\frac{2*\chi_{i-1,j}\chi_{i,j}}{\chi_{i-1,j}+\chi_{i,j}}$$

depends implicitly on the material temperature T.

3.2 Construction of implicit interface fluxes $F_{i-1/2,j,m}$ and $H_{i,j-1/2,m}$

Different from the explicit approaches in [10,12,14,15], where the interface fluxes $F_{i-1/2,j,m}$ and $H_{i,j-1/2,m}$ in Eq. (3.3) depend only on the initial value of intensity I, the IUGKS will construct the fluxes $F_{i-1/2,j,m}$ and $H_{i,j-1/2,m}$ implicitly. First, for the x-direction flux $F_{i-1/2,j,m}$, the following initial value problem is solved at the cell interface $x=x_{i-1/2}$, $y=y_j$:

$$\begin{cases}\dfrac{\epsilon}{c}\partial_t I_m+\mu_m\partial_x I_m=\mathcal{L}^{\epsilon}_a\sigma_a\left(\dfrac{1}{2\pi}\phi-I_m\right)+\mathcal{L}^{\epsilon}_s\sigma_s\left(\dfrac{1}{2\pi}\rho-I_m\right),\\ I_m(x,y_j,t)|_{t=t^n}=I_{m,0}(x,y_j).\end{cases} \tag{3.4}$$

A time dependent solution can be obtained as follows,

$$\begin{aligned}I_m(t,x_{i-1/2},y_j,\mu_m,\xi_m)=&e^{-\nu_{i-1/2,j}(t-t^n)}I_{m,0}\left(x_{i-1/2}-\frac{c\mu_m}{\epsilon}(t-t^n)\right)\\&+\int_{t^n}^{t}e^{-\nu_{i-1/2,j}(t-s)}\left(\frac{c\mathcal{L}^{\epsilon}_a\sigma_{a,i-1/2,j}}{2\pi\epsilon}\phi+\frac{c\mathcal{L}^{\epsilon}_s\sigma_{s,i-1/2,j}}{2\pi\epsilon}\rho\right)\left(s,x_{i-1/2}-\frac{c\mu_m}{\epsilon}(t-s)\right)ds,\end{aligned} \tag{3.5}$$

https://doi.org/10.4208/cicp.OA-2016-0261 Published online by Cambridge University Press

where $\nu=c(\mathcal{L}_a^\epsilon\sigma_a+\mathcal{L}_s^\epsilon\sigma_a)/\epsilon$, and $\nu_{i-1/2,j}$ denotes the value of ν at the corresponding cell interface. Substituting $I_m(t,x_{i-1/2},y_j,\mu_m,\xi_m)$ in (3.5) to (3.3) and integrating it with respect to time t from t^n to t^{n+1}, the numerical flux $F_{i-1/2,j,m}$ in the x-direction can be determined. The numerical flux $H_{i,j-1/2,m}$ in the y-direction can be obtained in the same procedure.

In order to fully determine the solution in Eq. (3.5), it requires to determine the unknown functions, i.e., $I_{m,0}(x,y_j)$ as the initial condition, and $\phi(t,x,y)$, and $\rho(t,x,y)$ between the time t^n and t^{n+1} around the cell interface $(x_{i-1/2},y_j)$. The function $I_{m,0}(x,y_j)$ in (3.4) can be reconstructed implicitly by a piecewise linear function:

$$I_{m,0}(x,y_j)=\begin{cases} I^{n+1}_{i-1,j,m}+\delta_x I^{n+1}_{i-1,j,m}(x-x_{i-1}), & \text{if } x<x_{i-1/2},\\ I^{n+1}_{i,j,m}+\delta_x I^{n+1}_{i,j,m}(x-x_i), & \text{if } x>x_{i-1/2}. \end{cases} \tag{3.6}$$

Here $\delta_x I^{n+1}_{i-1,j,m}$,$\delta_x I^{n+1}_{i,j,m}$ are the slopes which can be obtained from three unknowns $I^{n+1}_{i-1,j,m}$, $I^{n+1}_{i,j,m}$, $I^{n+1}_{i+1,j,m}$ with an implementation of the MUSCL slope limiter [11] to avoid spurious oscillations. For the function $\phi(x,y_j,t)$ between the time steps t^n and t^{n+1} around the cell interface $(x_{i-1/2},y_j)$, a piecewise continuous polynomial is used for its solution,

$$\phi(x,y_j,t)=\phi^{n+1}_{i-1/2,j}+\delta_t\phi^{n+1}_{i-1/2,j}(t-t^{n+1})+\begin{cases} \delta_x\phi^{n+1,L}_{i-1/2,j}(x-x_{i-1/2}), & \text{if } x<x_{i-1/2},\\ \delta_x\phi^{n+1,R}_{i-1/2,j}(x-x_{i-1/2}), & \text{if } x>x_{i-1/2}. \end{cases} \tag{3.7}$$

Here $\phi^{n+1}_{i-1/2,j}$ is the cell interface value, and the one-sided finite difference approximations are given by

$$\delta_x\phi^{n+1,L}_{i-1/2,j}=\frac{\phi^{n+1}_{i-1/2,j}-\phi^{n+1}_{i-1,j}}{\Delta x/2},\quad \delta_x\phi^{n+1,R}_{i-1/2,j}=\frac{\phi^{n+1}_{i,j}-\phi^{n+1}_{i-1/2,j}}{\Delta x/2}.$$

The time derivative $\delta_t\phi^{n+1}_{i-1/2,j}$ is discretized as

$$\delta_t\phi^{n+1}_{i-1/2,j}=\frac{\phi^{n+1}_{i-1/2,j}-\phi^{n}_{i-1/2,j}}{\Delta t},$$

where $\phi^{n+1}_{i-1/2,j}$,$\phi^{n+1}_{i-1,j}$,$\phi^{n+1}_{i,j}$ will be determined by the method in Subsection 3.3. The function $\rho(x,y_j,t)$ between the time steps t^n and t^{n+1} around the cell interface $(x_{i-1/2},y_j)$ can be determined similarly as in (3.7) with ϕ being replaced by ρ. The interface flux in the y-direction is constructed similarly. This completes the construction of the numerical scheme for Eq. (3.2).

In order to fully determine the interface intensity in (3.5) for flux evaluation, the macro variables ϕ and ρ in Eq. (3.7) need to be determined first. Their calculations will be presented in the next subsection. Here, we first present the detailed numerical flux function $F_{i-1/2,j,m}$ in the x-direction. Given the above constructions, the flux becomes

$$F_{i-1/2,j,m}=\frac{c\mu_m}{\epsilon\Delta t}\int_{t^n}^{t^{n+1}} I_m(t,x_{i-1/2},y_j,\mu_m,\xi_m)dt,$$

https://doi.org/10.4208/cicp.OA-2016-0261 Published online by Cambridge University Press

which can be exactly computed using the expressions (3.5), (3.6), and (3.7). The detailed formulation is the following.

$$\begin{aligned}F_{i-1/2,j,m}=&A_{i-1/2,j}\mu_m(I^{n+1,-}_{i-1/2,j,m}1_{\mu_m>0}+I^{n+1,+}_{i-1/2,j,m}1_{\mu_m<0})+C^1_{i-1/2,j}\mu_m\phi^{n+1}_{i-1/2,j}\\&+C^2_{i-1/2,j}\mu_m\rho^{n+1}_{i-1/2,j}+D^1_{i-1/2,j}(\mu_m^2\delta_x\phi^{n+1,L}_{i-1/2,j}1_{\mu_m>0}+\mu_m^2\delta_x\phi^{n+1,R}_{i-1/2,j}1_{\mu_m<0})\\&+D^2_{i-1/2,j}(\mu_m^2\delta_x\rho^{n+1,L}_{i-1/2,j}1_{\mu_m>0}+\mu_m^2\delta_x\rho^{n+1,R}_{i-1/2,j}1_{\mu_m<0})\\&+B_{i-1/2,j}(\mu_m^2\delta_x I^{n+1}_{i-1,j,m}1_{\mu_m>0}+\mu_m^2\delta_x I^{n+1}_{i,j,m}1_{\mu_m<0})\\&+E^1_{i-1/2,j}\mu_m\delta_t\phi^{n+1}_{i-1/2,j}+E^2_{i-1/2,j}\mu_m\delta_t\rho^{n+1}_{i-1/2,j},\end{aligned}\tag{3.8}$$

where $I^{n+1,-}_{i-1/2,j,m}$, $I^{n+1,+}_{i-1/2,j,m}$ denote the interface values

$$I^{n+1,-}_{i-1/2,j,m}=I^{n+1}_{i-1,j,m}+\frac{\Delta x}{2}\delta_x I^{n+1}_{i-1,j,m},\quad I^{n+1,+}_{i-1/2,j,m}=I^{n+1}_{i,j,m}-\frac{\Delta x}{2}\delta_x I^{n+1}_{i,j,m}.$$

The coefficients in (3.8) are given by

$$A=\frac{c}{\epsilon\Delta t\nu}(1-e^{-\nu\Delta t}),\tag{3.9a}$$

$$C^1=\frac{c^2\mathcal{L}^\epsilon_a\sigma_a}{2\pi\Delta t\epsilon^2\nu}\left(\Delta t-\frac{1}{\nu}(1-e^{-\nu\Delta t})\right),\tag{3.9b}$$

$$C^2=\frac{c^2\mathcal{L}^\epsilon_s\sigma_s}{2\pi\Delta t\epsilon^2\nu}\left(\Delta t-\frac{1}{\nu}(1-e^{-\nu\Delta t})\right),\tag{3.9c}$$

$$D^1=-\frac{c^3\mathcal{L}^\epsilon_a\sigma_a}{2\pi\Delta t\epsilon^3\nu^2}\left(\Delta t(1+e^{-\nu\Delta t})-\frac{2}{\nu}(1-e^{-\nu\Delta t})\right),\tag{3.9d}$$

$$D^2=-\frac{c^3\mathcal{L}^\epsilon_s\sigma_s}{2\pi\Delta t\epsilon^3\nu^2}\left(\Delta t(1+e^{-\nu\Delta t})-\frac{2}{\nu}(1-e^{-\nu\Delta t})\right),\tag{3.9e}$$

$$B=-\frac{c^2}{\epsilon^2\nu^2\Delta t}(1-e^{-\nu\Delta t}-\nu\Delta te^{-\nu\Delta t}),\tag{3.9f}$$

$$E^1=\frac{c^2\mathcal{L}^\epsilon_a\sigma_a}{2\pi\epsilon^2\nu^3\Delta t}\left(1-e^{-\nu\Delta t}-\nu\Delta te^{-\nu\Delta t}-\frac{1}{2}(\nu\Delta t)^2\right),\tag{3.9g}$$

$$E^2=\frac{c^2\mathcal{L}^\epsilon_s\sigma_s}{2\pi\epsilon^2\nu^3\Delta t}\left(1-e^{-\nu\Delta t}-\nu\Delta te^{-\nu\Delta t}-\frac{1}{2}(\nu\Delta t)^2\right),\tag{3.9h}$$

with $\nu=c(\mathcal{L}^\epsilon_a\sigma_a+\mathcal{L}^\epsilon_s\sigma_a)/\epsilon$. The expressions (3.9) have functional dependence on physical coefficients, the time step, and asymptotic parameter,

$$A_{i-1/2,j}=A(\Delta t,\epsilon,\sigma_{a,i-1/2,j},\sigma_{s,i-1/2,j},\nu_{i-1/2,j}),\tag{3.10a}$$

$$C^1_{i-1/2,j}=C^1(\Delta t,\epsilon,\sigma_{a,i-1/2,j},\sigma_{s,i-1/2,j},\nu_{i-1/2,j}),\tag{3.10b}$$

$$C^2_{i-1/2,j}=C^2(\Delta t,\epsilon,\sigma_{a,i-1/2,j},\sigma_{s,i-1/2,j},\nu_{i-1/2,j}),\tag{3.10c}$$

$$D^1_{i-1/2,j}=D^1(\Delta t,\epsilon,\sigma_{a,i-1/2,j},\sigma_{s,i-1/2,j},\nu_{i-1/2,j}),\tag{3.10d}$$

https://doi.org/10.4208/cicp.OA-2016-0261 Published online by Cambridge University Press

$$D^2_{i-1/2,j} = D^2(\Delta t,\epsilon,\sigma_{a,i-1/2,j},\sigma_{s,i-1/2,j},\nu_{i-1/2,j}), \tag{3.10e}$$

$$B_{i-1/2,j} = B(\Delta t,\epsilon,\sigma_{a,i-1/2,j},\sigma_{s,i-1/2,j},\nu_{i-1/2,j}), \tag{3.10f}$$

$$E^1_{i-1/2,j} = E^1(\Delta t,\epsilon,\sigma_{a,i-1/2,j},\sigma_{s,i-1/2,j},\nu_{i-1/2,j}), \tag{3.10g}$$

$$E^2_{i-1/2,j} = E^2(\Delta t,\epsilon,\sigma_{a,i-1/2,j},\sigma_{s,i-1/2,j},\nu_{i-1/2,j}). \tag{3.10h}$$

Here we would like to point out that even with the interface solution (3.5), in order to obtain a consistent limiting diffusive flux, the coefficients in the evaluation (3.8), such as σ_a and σ_s at a cell interface, have to be properly defined using the values from neighboring cells.

3.3 Evolution solution of macroscopic governing equations

With the definition of $\phi = acT^4$ and $\rho = \int I d\vec{\Omega}$, the angle integration of the first equation in (2.1) give the following macroscopic system:

$$\begin{cases} \dfrac{\epsilon}{c}\dfrac{\partial \rho}{\partial t} + \nabla \cdot < \vec{\Omega} I > = \mathcal{L}^{\epsilon}_a \sigma_a (\phi - \rho), \\ C_v \dfrac{\partial T}{\partial t} \equiv \dfrac{\partial U}{\partial t} = \dfrac{\mathcal{L}^{\epsilon}_a \sigma_a}{\epsilon}(\rho - \phi) + \nabla \cdot (\chi \nabla T), \end{cases} \tag{3.11}$$

where the flux $< \vec{\Omega} I >$ is given by

$$< \vec{\Omega} I > = \int \vec{\Omega} I d\vec{\Omega}.$$

The macroscopic variables ρ and ϕ in (3.7) will be obtained by solving the system (3.11) iteratively. Here the system (3.11) in 2D case will be considered. The finite volume discretization for system (3.11) can be written as

$$\begin{cases} \rho^{n+1}_{i,j} = \rho^n_{i,j} + \dfrac{\Delta t}{\Delta x}(\Phi^{n+1}_{i-1/2,j} - \Phi^{n+1}_{i+1/2,j}) \\ \qquad\qquad + \dfrac{\Delta t}{\Delta y}(\Psi^{n+1}_{i,j-1/2} - \Psi^{n+1}_{i,j+1/2}) + \dfrac{\mathcal{L}^{\epsilon}_a \sigma^{n+1}_{a,i,j}}{\epsilon} c\Delta t(\phi^{n+1}_{i,j} - \rho^{n+1}_{i,j}), \\ C_v T^{n+1}_{i,j} = C_v T^n_{i,j} + \dfrac{\mathcal{L}^{\epsilon}_a \sigma^{n+1}_{a,i,j}}{\epsilon}\Delta t(\rho^{n+1}_{i,j} - \phi^{n+1}_{i,j}) + \dfrac{\Delta t}{\Delta x}(M_{i+1/2,j} - M_{i-1/2,j}) \\ \qquad\qquad + \dfrac{\Delta t}{\Delta y}(M_{i,j+1/2} - M_{i,j-1/2}), \end{cases} \tag{3.12}$$

where the material temperature diffusion operators are the same as that in (3.2), and the

https://doi.org/10.4208/cicp.OA-2016-0261 Published online by Cambridge University Press

cell interface fluxes Φ and Ψ for radiation energy are given by

$$\Phi^{n+1}_{i-1/2,j}=\frac{c}{\epsilon\Delta t}\int_{t^n}^{t^n+\Delta t}<\Omega_x I>(x_{i-1/2},y_j,t)dt, \tag{3.13a}$$

$$\Phi^{n+1}_{i+1/2,j}=\frac{c}{\epsilon\Delta t}\int_{t^n}^{t^n+\Delta t}<\Omega_x I>(x_{i+1/2},y_j,t)dt, \tag{3.13b}$$

$$\Psi^{n+1}_{i,j-1/2}=\frac{c}{\epsilon\Delta t}\int_{t^n}^{t^n+\Delta t}<\Omega_y I>(x_i,y_{j-1/2},t)dt, \tag{3.13c}$$

$$\Psi^{n+1}_{i,j+1/2}=\frac{c}{\epsilon\Delta t}\int_{t^n}^{t^n+\Delta t}<\Omega_y I>(x_i,y_{j+1/2},t)dt. \tag{3.13d}$$

The above flux functions depend on the radiation intensity I at the cell interface, which is given as follows. For example, at the left cell interface of cell i in the x-direction, we can use (3.5) and (3.8) to get

$$\begin{aligned}\Phi^{n+1}_{i-1/2,j}&=\frac{c}{\epsilon\Delta t}\int_{t^n}^{t^n+\Delta t}<\Omega_x I>(x_{i-1/2},y_j,t)dt\\&=\sum_{m=1}^{M}\omega_m F_{i-1/2,j,m}\\&=A^{n+1}_{i-1/2,j}\sum_{m=1}^{M}\omega_m\mu_m(I^{n+1,-}_{i-1,j,m}1_{\mu_m>0}+I^{n+1,+}_{i,j,m}1_{\mu_m<0})\\&\quad+\frac{2\pi D^{1,n+1}_{i-1/2,j}}{3}\left(\frac{\phi^{n+1}_{i,j}-\phi^{n+1}_{i-1,j}}{\Delta x}\right)+\frac{2\pi D^{2,n+1}_{i-1/2,j}}{3}\left(\frac{\rho^{n+1}_{i,j}-\rho^{n+1}_{i-1,j}}{\Delta x}\right)\\&\quad+B^{n+1}_{i-1/2,j}\sum_{m=1}^{M}\omega_m\mu_m^2(\delta_x I^{n+1}_{i-1,j,m}1_{\mu_m>0}+\delta_x I^{n+1}_{i,j,m}1_{\mu_m<0}),\end{aligned} \tag{3.14}$$

where the parameters $A^{n+1}_{i-1/2,j}$, $B^{n+1}_{i-1/2,j}$, $D^{1,n+1}_{i-1/2,j}$, and $D^{2,n+1}_{i-1/2,j}$ in (3.14) have the same functional dependence as the parameters $A_{i-1/2,j}$, $B_{i-1/2,j}$, $D^1_{i-1/2,j}$, $D^2_{i-1/2,j}$ in (3.10). The cell interface parameters $\sigma_{a,i-1/2,j}$ and $\sigma_{s,i-1/2,j}$ take values

$$\sigma^{n+1}_{a,i-1/2,j}=\frac{2\sigma^{n+1}_{a,i,j}\sigma^{n+1}_{a,i-1,j}}{\sigma^{n+1}_{a,i,j}+\sigma^{n+1}_{a,i-1,j}},$$

and

$$\sigma^{n+1}_{s,i-1/2,j}=\frac{2\sigma^{n+1}_{s,i,j}\sigma^{n+1}_{s,i-1,j}}{\sigma^{n+1}_{s,i,j}+\sigma^{n+1}_{s,i-1,j}}.$$

The expression for the interface fluxes $\Phi^{n+1}_{i+1/2,j}$, $\Psi^{n+1}_{i,j-1/2}$, and $\Psi^{n+1}_{i,j+1/2}$, can be obtained similarly.

https://doi.org/10.4208/cicp.OA-2016-0261 Published online by Cambridge University Press

Thus, with the given interface fluxes, Eq. (3.12) become a coupled nonlinear system for the macro variables $\phi_{i,j}^{n+1}$ and $\rho_{i,j}^{n+1}$, where the parameters $\sigma_{a,i,j}^{n+1}$ and $\sigma_{s,i,j}^{n+1}$ depend implicitly on the material temperature $T_{i,j}^{n+1}$. This nonlinear system can be solved by an iterative method, which is coupled with the radiation transfer equations (3.2), since the macroscopic fluxes $\Phi_{i-1/2,j}^{n+1}$ depend on the intensity I and its slopes implicitly.

3.4 IUGKS for the radiative transfer system

With the assumption of the known radiation intensity $I_{i,j,m}$ and its slopes $\delta_x I_{i,j,m}^{n+1}$ in (3.12), $\phi_{i,j}^{n+1}$ and $\rho_{i,j}^{n+1}$ can be determined through an iterative method. Taking the values of

$$\tilde{\phi}_{i,j}=\phi_{i,j}^{n+1},\quad \tilde{\rho}_{i,j}=\rho_{i,j}^{n+1}$$

in (3.2), the cell interface value $\phi_{i-1/2,j}^{n+1}$ in (3.7) becomes

$$\begin{cases} \phi_{i-1/2,j}^{n+1}=\dfrac{1}{2}(\phi_{i-1,j}^{n+1}+\phi_{i,j}^{n+1}), \\ \rho_{i-1/2,j}^{n+1}=\dfrac{1}{2}(\rho_{i-1,j}^{n+1}+\rho_{i,j}^{n+1}). \end{cases} \tag{3.15}$$

The parameters $\sigma_{a,i-1/2,j}$ and $\sigma_{s,i-1/2,j}$ in (3.10) are determined by

$$\sigma_{a,i-1/2,j}^{n+1}=\frac{2\sigma_{a,i,j}^{n+1}\sigma_{a,i-1,j}^{n+1}}{\sigma_{a,i,j}^{n+1}+\sigma_{a,i-1,j}^{n+1}}$$

and

$$\sigma_{s,i-1/2,j}^{n+1}=\frac{2\sigma_{s,i,j}^{n+1}\sigma_{s,i-1,j}^{n+1}}{\sigma_{s,i,j}^{n+1}+\sigma_{s,i-1,j}^{n+1}}$$

respectively with the updated material temperature $T_{i,j}^{n+1}$ in (3.12). Thus, the interface flux for the first equation of the system (3.2) is fully obtained, such as the determination of $F_{i-1/2,j}$ by formula (3.8), which depends on the assumed values $I_{i,j,m}^{n+1}$ and $I_{i-1,j,m}^{n+1}$. The remaining fluxes $F_{i+1/2,j}$, $H_{i,j-1/2}$ and $H_{i,j+1/2}$ can be obtained similarly. Therefore, the first equation in (3.2) can be solved by the following implicit scheme

$$\begin{aligned} I_{i,j,m}^{n+1}=&I_{i,j,m}^{n}+\frac{\Delta t}{\Delta x}(F_{i-1/2,j}-F_{i+1/2,j})+\frac{\Delta t}{\Delta y}(H_{i,j-1/2}-H_{i,j+1/2}) \\ &+c\Delta t\frac{\mathcal{L}_a^{\epsilon}\sigma_{a,i,j}^{n+1}}{\epsilon}\left(\frac{1}{2\pi}\phi_{i,j}^{n+1}-I_{i,j,m}^{n+1}\right)+\frac{c\Delta t\mathcal{L}_s^{\epsilon}\sigma_{s,i,j}^{n+1}}{\epsilon}\left(\frac{1}{2\pi}\rho_{i,j}^{n+1}-I_{i,j,m}^{n+1}\right). \end{aligned} \tag{3.16}$$

The final step is to solve the second equation in (3.2) to obtain the final material temperature $T_{i,j}^{n+1}$ with the newly obtained value $I_{i,j,m}^{n+1}$. The solution of the temperature can

https://doi.org/10.4208/cicp.OA-2016-0261 Published online by Cambridge University Press

be directly obtained by solving the implicit equation,

$$C_v\frac{T_{i,j}^{n+1}-T_{i,j}^{n}}{\Delta t}=\frac{\mathcal{L}_a^{\epsilon}\sigma_a}{\epsilon}\Big(\sum_{m=1}^{M}\omega_m\tilde{I}_{i,j,m}-\tilde{\phi}_{i,j}\Big)+\frac{1}{\Delta x}(M_{i+1/2,j}-M_{i-1/2,j})$$
$$+\frac{1}{\Delta y}(M_{i,j+1/2}-M_{i,j-1/2}). \tag{3.17}$$

Based on (3.17), through an iterative method the material temperature $T_{i,j}^{n+1}$ is obtained. The above numerical procedure can be repeated iteratively and this completes the construction of IUGKS for the gray radiation transfer system (2.1) with strong scattering. We summarize the steps of IUGKS in the following.

Loop of IUGKS: Given $I_{i,j,m}^{n}$ and $T_{i,j}^{n}$, we have $\rho_{i,j}^{n}$ and $\phi_{i,j}^{n}$. Find $I_{i,j,m}^{n+1}$ and $T_{i,j}^{n+1}$.

1) Let $T^{n+1,0}=T^{n}$, $I_{i,j,m}^{n+1,0}=I_{i,j,m}^{n}$;

2) For $s=1,\cdots,S$

{

2.1) With $I_{i,j,m}^{n+1}=I_{i,j,m}^{n+1,s-1}$, use (3.14) to calculate the macro flux. Solve the system (3.12) to obtain $\phi_{i,j}^{n+1}$,$\rho_{i,j}^{n+1}$;

2.2) With the obtained value $\phi_{i,j}^{n+1}$ and $\rho_{i,j}^{n+1}$ from the above step, solve the resulting equation (3.16) implicitly for $I_{i,j,m}^{n+1,s}$;

2.3) With the solution $I_{i,j,m}^{n+1,s}$, solve (3.17) to get the new material temperature $T_{i,j}^{n+1,s}$.

2.4) Calculate the iteration error, exit when convergence.

}

3) Assigning $T_{i,j}^{n+1}=T_{i,j}^{n+1,s}$,$I_{i,j,m}^{n+1}=I_{i,j,m}^{n+1,s}$, go to next computational step.

End

It should be pointed out that in the above algorithm of IUGKS, the steps 2.1), 2.2) and 2.3) are needed to solve the implicit system by iteration method. In this paper, these three equations are solved by the Gauss-Sedel iterative method.

4 Asymptotic preserving property of IUGKS

For radiative transfer methods, to have the asymptotic preserving (AP) property is important for any scheme [4–8]. For the equilibrium limit case with $\mathcal{L}_a^{\epsilon}=1/\epsilon$ and $\mathcal{L}_s^{\epsilon}=\epsilon$, the asymptotic preserving analysis is similar to that in the previous papers [14, 15]. This is omitted here. But, for the non-equilibrium case, in the small ϵ limit we will show its asymptotic property. In the above IUGKS, the coefficients in the scheme takes the following limiting values.

https://doi.org/10.4208/cicp.OA-2016-0261 Published online by Cambridge University Press

Proposition 4.1. *Let σ_a and σ_s be positive, and $\mathcal{L}_a^\epsilon=\epsilon$ and $\mathcal{L}_s^\epsilon=1/\epsilon$. As ϵ tends to zero, we have*

- $A(\Delta t,\epsilon,\sigma_a,\sigma_s)$ *tends to 0;*
- $B(\Delta t,\epsilon,\sigma_a,\sigma_s)$ *tends to 0;*
- $D^1(\Delta t,\epsilon,\sigma_a,\sigma_s)$ *tends to 0;*
- $D^2(\Delta t,\epsilon,\sigma_a,\sigma_s)$ *tends to* $-c/(2\pi\sigma_s)$.

Thus, based on Proposition 1, the corresponding macroscopic diffusion flux $(\text{Diff})_{i-1/2,j}^{n+1}$ defined by

$$\begin{aligned}(\text{Diff})_{i-1/2,j}^{n+1}&=\left\langle\frac{c\mu}{\epsilon\Delta t}\int_{t^n}^{t^{n+1}}I(t,x_{i-1/2},y_j,\mu,\xi)dt\right\rangle\\&=\int\frac{c\mu}{2\pi\epsilon\Delta t}\int_{t^n}^{t^{n+1}}I(t,x_{i-1/2},y_j,\mu,\xi)dtd\mu d\xi,\end{aligned}\tag{4.1}$$

has the following limit:

$$\begin{aligned}(\text{Diff})_{i-1/2,j}^{n+1}&=\frac{1}{2\pi}\sum_{m=1}^{M}\omega_m\mu_m I_m(t,x_{i-1/2},y_j,\mu_m,\xi_m)\\&\xrightarrow[\epsilon\to0]{}-\left(\frac{c}{6\sigma_{s,i-1/2,j}}\delta_x\rho_{i-1/2,j}^{n+1,L}+\frac{c}{6\sigma_{s,i-1/2,j}}\delta_x\rho_{i-1/2,j}^{n+1,R}\right)\\&=-\frac{c}{3\sigma_{s,i-1/2,j}}\frac{\rho_{i,j}^{n+1}-\rho_{i-1,j}^{n+1}}{\Delta x}.\end{aligned}\tag{4.2}$$

The limiting solution in Eq. (4.2) gives the numerical flux of the first asymptotic limiting equations (2.3), which is the standard three points scheme for the diffusion equation in the one-dimensional case, and the five points scheme in the two-dimensional case.

Now, based on IUGKS for the radiation transfer equation (3.1), the current scheme is indeed asymptotic preserving. This is given by the following proposition.

Proposition 4.2. *Let σ_a and σ_s be positive, $\mathcal{L}_a^\epsilon=\epsilon$ and $\mathcal{L}_s^\epsilon=1/\epsilon$. Then as ϵ tends to zero, the numerical scheme given by* (3.12), (3.16), *and* (3.17) *approaches to the standard implicit diffusion scheme for the non-equilibrium diffusion limit system* (2.3).

Proof. Firstly, on the order ϵ^{-2} in (3.16), as the parameter ϵ tends to zero, we have

$$I_{i,j,m}^{n+1}\to\frac{1}{2\pi}\rho_{i,j}^{n+1},$$

which shows an isotropic limit intensity in the limiting case. If we integrate both sides of this equation with respect to the angle variable, then as $\epsilon\to0$, we find that

$$\sum_{m=1}^{N}I_{i,j,m}^{n+1}\omega_m\to\rho_{i,j}^{n+1}.\tag{4.3}$$

https://doi.org/10.4208/cicp.OA-2016-0261 Published online by Cambridge University Press

Secondly, on the order ϵ^{-1} in (3.16), with the flux $F^{n+1}_{i-1/2,j}$ given by (3.8), the integration of the flux $F^{n+1}_{i-1/2,j}$ over the angle variable gives the macro flux $\Phi^{n+1}_{i-1/2,j}$ in the expression (3.14). By Proposition 1, as $\epsilon \to 0$, we have

$$\Phi^{n+1}_{i-1/2,j} \to -\frac{c}{3\sigma^{n+1}_{s,i-1/2,j}} \frac{\rho^{n+1}_{i,j} - \rho^{n+1}_{i-1,j}}{\Delta x}. \tag{4.4}$$

Similarly, as the parameter $\epsilon \to 0$, the other interface fluxes for macroscopic quantities transport go to

$$\Phi^{n+1}_{i+1/2,j} \to -\frac{c}{3\sigma^{n+1}_{s,i+1/2,j}} \frac{\rho^{n+1}_{i,j} - \rho^{n+1}_{i+1,j}}{\Delta x}, \tag{4.5a}$$

$$\Psi^{n+1}_{i,j-1/2} \to -\frac{c}{3\sigma^{n+1}_{s,i,j-1/2}} \frac{\rho^{n+1}_{i,j} - \rho^{n+1}_{i,j-1}}{\Delta y}, \tag{4.5b}$$

$$\Psi^{n+1}_{i,j+1/2} \to -\frac{c}{3\sigma^{n+1}_{s,i,j+1/2}} \frac{\rho^{n+1}_{i,j} - \rho^{n+1}_{i,j+1}}{\Delta y}. \tag{4.5c}$$

Thirdly, if we integrate Eq. (3.16) with respect to the angle variable, as the parameter $\epsilon \to 0$, we get

$$\begin{aligned}\rho^{n+1}_{i,j} =& \rho^{n}_{i,j} + \frac{\Delta t}{\Delta x}\left(-\frac{c}{3\sigma^{n+1}_{i-1/2,j}} \frac{\Phi^{n+1}_{i,j} - \Phi^{n+1}_{i-1,j}}{\Delta x} + \frac{c}{3\sigma^{n+1}_{i+1/2,j}} \frac{\Phi^{n+1}_{i,j} - \Phi^{n+1}_{i+1,j}}{\Delta x} \right) \\ &+ \frac{\Delta t}{\Delta y}\left(-\frac{c}{3\sigma^{n+1}_{i,j-1/2}} \frac{\Phi^{n+1}_{i,j} - \Phi^{n+1}_{i,j-1}}{\Delta y} + \frac{c}{3\sigma^{n+1}_{i,j+1/2}} \frac{\Phi^{n+1}_{i,j} - \Phi^{n+1}_{i,j+1}}{\Delta y} \right) - c\sigma_a(\rho^{n+1}_{i,j} - \phi^{n+1}_{i,j}).\end{aligned} \tag{4.6}$$

At the same time, from the material temperature discretization in Eqs. (3.12), (3.16), and (3.17), we can observe by (4.3) that the second equation of (2.3) is discretized correctly independent of the parameter ϵ. Thus, the convergence of the material temperature equation is automatically satisfied.

Eq. (4.6) is a standard five points scheme for the first diffusion limit equation (2.3). This indicates that IUGKS for the radiative transfer system (2.1) is an asymptotic preserving (AP) method. □

5 Extension to frequency-dependent radiative transfer system

The IUGKS introduced above can be used to solve the frequency-dependent radiation transfer system as well. The system can be written in the following scaled form,

https://doi.org/10.4208/cicp.OA-2016-0261 Published online by Cambridge University Press

$$\begin{cases} \dfrac{\epsilon}{c}\dfrac{\partial I}{\partial t}+\vec{\Omega}\cdot\nabla I=\mathcal{L}_a^\epsilon\sigma_a(B(\nu,T)-I)+\mathcal{L}_s^\epsilon\sigma_s\Big(\dfrac{1}{4\pi}\displaystyle\int_{4\pi}Id\vec{\Omega}-I\Big), \\ C_v\dfrac{\partial T}{\partial t}\equiv\dfrac{\partial U}{\partial t}=\dfrac{\mathcal{L}_a^\epsilon\sigma_a}{\epsilon}\displaystyle\int_{4\pi}\int_0^\infty\Big(I-B(\nu,T)\Big)d\nu d\vec{\Omega}. \end{cases} \tag{5.1}$$

Here $I(t,\vec{r},\vec{\Omega},\nu)$ is the radiation intensity at frequency ν with $\nu\in(0,+\infty)$. The Planck function $B(\nu,T)$ is given by

$$B(\nu,T)=\frac{2h\nu^3}{c^2}\frac{1}{e^{h\nu/kT}-1}, \tag{5.2}$$

where h is Planck's constant and k is Boltzmann's constant. Following the approach in paper [15], we first use the multi-group method to discretize the frequency variable ν in the system (5.1), and obtain the multi-group equations. Then, the IUGKS presented in this paper can be extended to solve multi-group system, where the equation at each frequency is similar to what we have solved before. The numerical examples will include the IUGKS solution for the above frequency-dependent system.

6 Numerical experiments

For the system (2.1) with strong scattering, two problems will be studied in the following. The paper [16] provided the description for the non-equilibrium diffusion case. The problems tested are the hard and easy transient cases. The hard transient is the one that has steep gradients and a wide range of time scales. The easy problem is one that has mild gradients and an almost fixed time scale. For system (5.1) with strong absorption/emission, we will use the Larsen's test Problem in [15,17,18] to test the performance of the implicit method. For explicit UGKS simulation, the time step is determined by $\Delta t=CFL*min(\Delta x,\Delta y)/c$, and the Courant number CFL takes a value of 0.9 in the following numerical testing. For the IUGKS simulations, we introduce the time-step enlarging factor $f_e=1.2$ and shortening factor $f_s=0.8$. For the first time step, we take $CFL=5.0$ for simplicity, and then the implicit time step can be enlarged or shortened with the factor f_e or f_s in terms of the iteration number s in the Loops of the IUGKS. For the problems in this paper, we take the maximum iteration number $S=13$. If $s\leq 8$, we can enlarge the time step for the next iterative level by a factor f_e. When $9\leq s\leq 12$, the time step for the next iterative level is unchanged. For the non-convergent case even at $s=S$, the time step is shortened by a factor f_s until convergence. We take $\mathcal{L}_a^\epsilon=1.0/\epsilon$ and $\mathcal{L}_s^\epsilon=0.0$ to study the strong absorption/emission case in the first one dimensional problem, and we take $\mathcal{L}_a^\epsilon=\epsilon$ and $\mathcal{L}_s^\epsilon=1.0/\epsilon$ in the last two examples to consider the strong scattering phenomena.

Example 6.1 (Larsen's Test Problem [15,17,18])**.** For this problem, the frequency variable ν is logarithmaically spaced with 50 groups between $h\nu_{\min}=10^{-5}keV$ and $h\nu_{\max}=10keV$.

https://doi.org/10.4208/cicp.OA-2016-0261 Published online by Cambridge University Press

Group g is defined by $\nu_{g-\frac{1}{2}} \le \nu \le \nu_{g+\frac{1}{2}}$, where

$$\nu_{\frac{1}{2}} = \nu_{\min}, \quad \nu_{g+\frac{1}{2}} = \left(\frac{\nu_{\max}}{\nu_{\min}}\right)^{\frac{1}{50}} \nu_{g-\frac{1}{2}}.$$

The computational domain is divided into three regions with different cell sizes,

$$\Delta x = \begin{cases} 0.10\,cm, & 0\,cm < x < 1\,cm, \\ 0.02\,cm, & 1\,cm < x < 2\,cm, \\ 0.20\,cm, & 2\,cm < x < 4\,cm. \end{cases}$$

The opacity models photo-ionization absorption,

$$\sigma(\nu,T,x) = \gamma(x)\frac{1-e^{-h\nu/kT}}{(h\nu)^3},$$

where

$$\gamma(x) = \begin{cases} 1keV^3/cm, & 0\,cm < x < 1\,cm, \\ 1000keV^3/cm, & 1\,cm < x < 2\,cm, \\ 1keV^3/cm, & 2\,cm < x < 4\,cm. \end{cases}$$

The heat capacity C_v keeps a constant value $5.109\times10^{14} erg\cdot keV^{-1}\,cm^{-3}$. The initial material temperature is given by $T(x,0) = 10^{-3}keV$, which is in equilibrium with the initial radiation intensity. No radiation enters from the left boundary, but a steady, direction-dependent, $1keV$ Planckian distribution of photons enters from the right boundary. The simulation runs up to a time of $900ps$. Fig. 1 shows the results computed by the IUGKS, UGKS, and IMC (implicit Monte Carlo) method [2]. Small differences appear between IUGKS and IMC solutions in opacity thin regions. The computational cost of IUGKS for this case is about 1 minute with $N=4$, and 15 minute with $N=12$ in a personal notebook. It takes IMC 63 minutes for the same computer. In order to identify the effect of the angle discretization, in Fig. 2 the results from three different angle discretizations are given. In Fig. 3, the results of material and radiation temperature are given with mesh refinement.

Example 6.2 (Hard Problem)**.** The hard test problem is solved on a domain $[0,1]\times[0,1]$ with a Cartesian mesh $\Delta x = \Delta y$. The absorption and scattering coefficients are modeled by

$$\sigma_a(x,y,T) = \sigma_s(x,y,T) = \frac{Z(x,y)^3}{T^3}.$$

The function Z is 10 inside two obstacles which are defined by $[\frac{3}{16},\frac{7}{16}]\times[\frac{9}{16},\frac{13}{16}]$ and $[\frac{9}{16},\frac{13}{16}]\times[\frac{3}{16},\frac{7}{16}]$, and Z is 1 at other places. All four boundaries are insulate for material temperature, and for radiation transfer the left and lower boundaries are reflective, the right and upper boundaries are outflow. In this test case, for simplicity, we set the constants $a=c=1$. The initial value of radiation intensity has the form of $I_0 = \frac{E(r)}{2\pi}$, where

$$E(r) = 0.001 + 100\exp\left[-\left(\frac{r}{0.1}\right)^2\right],$$

https://doi.org/10.4208/cicp.OA-2016-0261 Published online by Cambridge University Press

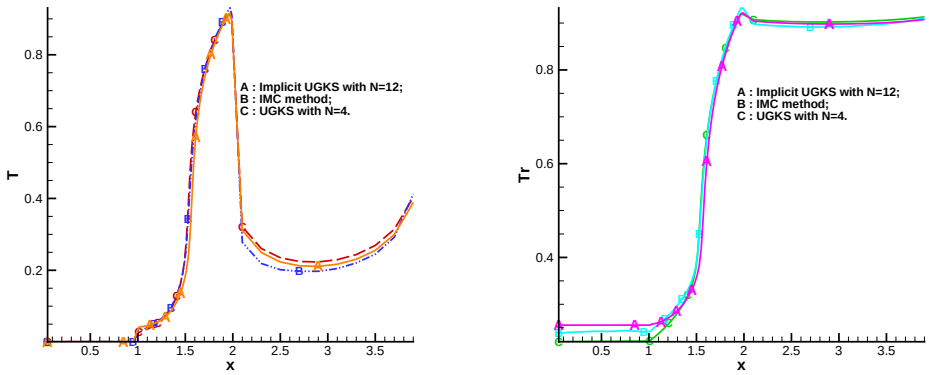


Figure 1: Results of Larsen's tests (Example 6.1) at $900ps$ computed by IUGKS, UGKS, and IMC (implicit Monte Carlo) method. Left: material temperature; Right: radiation temperature.

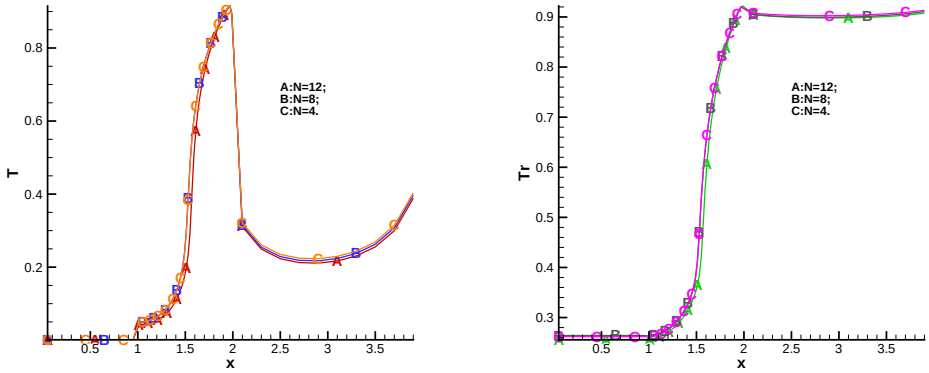


Figure 2: IUGKS results with different angle discretization.

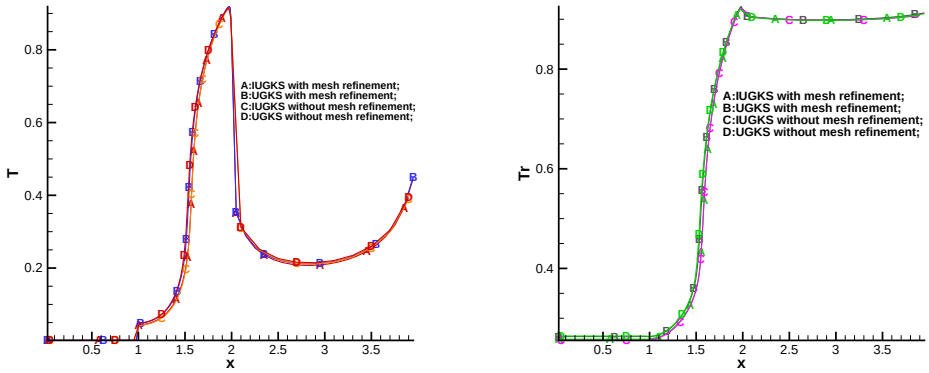


Figure 3: IUGKS and UGKS results with spatial mesh refinement.

https://doi.org/10.4208/cicp.OA-2016-0261 Published online by Cambridge University Press

where $r=\sqrt{x^2+y^2}$ is the distance from the origin, which is located in the lower left corner of the computational domain. The initial material temperature is given by

$$T(x,y)=E(x,y)^{1/4}.$$

We test this problem with $\epsilon=10^{-6}$ and $\epsilon=10^{-2}$ in (2.1). The contours of the material and radiation temperature at five different times $t=0.6,1.2,1.8,2.4$, and 3, are shown in Fig. 4 for $\epsilon=10^{-6}$ and in Fig. 5 for $\epsilon=10^{-2}$ respectively. From which we can see that material temperature and radiation temperature are quite different in the process of time evolution. This also shows the non-equilibrium effect of the strong scattering phenomena.

Example 6.3 (Easy Problem)**.** The easy test problem is solved on a domain $[0,2]\times[0,1]$ with a Cartesian mesh $\Delta x=\Delta y$. The absorption and scattering coefficients are the same as

$$\sigma_a(x,y,T)=\sigma_s(x,y,T)=\frac{Z(x,y)^3}{T^3}.$$

The function Z is 1.5 in two obstacles which are defined by $[\frac{3}{16},\frac{13}{16}]\times[\frac{3}{16},\frac{13}{16}]$ and $[\frac{19}{16},\frac{29}{16}]\times[\frac{3}{16},\frac{13}{16}]$, and Z is 1 otherwise. All four boundaries are insulate for material temperature. But for radiation transfer, the left boundary has an incident intensity with $I|_{x=0}=\frac{5}{4\pi}$, the lower and upper boundaries are reflective, and the right one is outflow. In this test case, for simplicity we set the constants $a=c=1$. The initial value of radiation intensity takes the form $I_0=\frac{E(x,y)}{2\pi}$, where

$$E(x,y)=0.001.$$

The initial material temperature is given by

$$T(x,y)=E(x,y)^{1/4}.$$

The problem is tested with the parameter $\epsilon=10^{-6}$ and $\epsilon=10^{-2}$ for system (2.1). The contours of the material and radiation temperature at five different time $t=0.6,1.2,1.8,2.4$, and 3.0 are shown in Fig. 6 for $\epsilon=10^{-6}$ and in Fig. 7 for $\epsilon=10^{-2}$ respectively. From which we can observe the differences in the material and radiation temperature evolution in the non-equilibrium case.

7 Conclusion

In this paper, the UGKS is extended to solve radiative transfer system with both scattering and absorption/emission effects. At the same time, an implicit UGKS is developed. In the proposed IUGKS, due to the implicit treatment in the flux function, the CFL constraint can be released. As a result, the computational efficiency can be much improved in comparison with the explicit UGKS. At the same time, the current IUGKS has the asymptotic preserving (AP) property, where depending on the scaling of absorption/emission

https://doi.org/10.4208/cicp.OA-2016-0261 Published online by Cambridge University Press

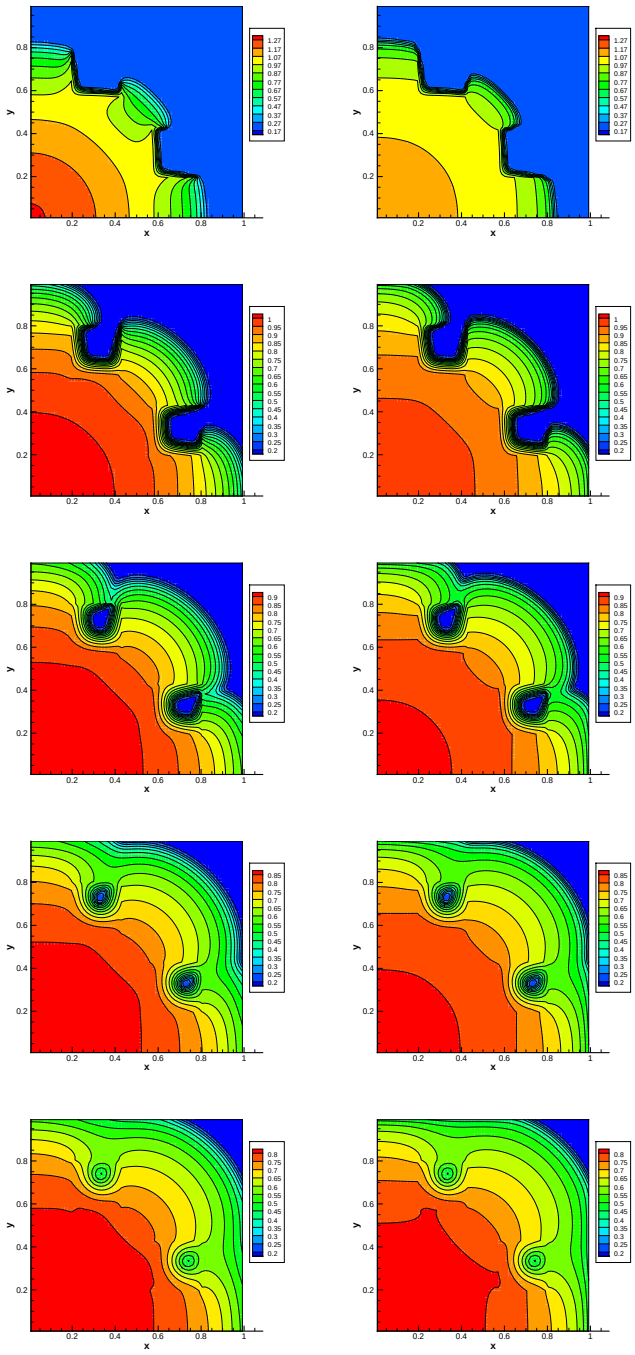


Figure 4: Hard problem (Example 6.1) with parameter $\epsilon = 10^{-6}$ for material temperature on the left, and radiation temperature on the right. At five output times $t = 0.6, 1.2, 1.8, 2.4$, and 3.0 from top to bottom. There are material temperature and radiation temperature differences in the evolution process.

https://doi.org/10.4208/cicp.OA-2016-0261 Published online by Cambridge University Press

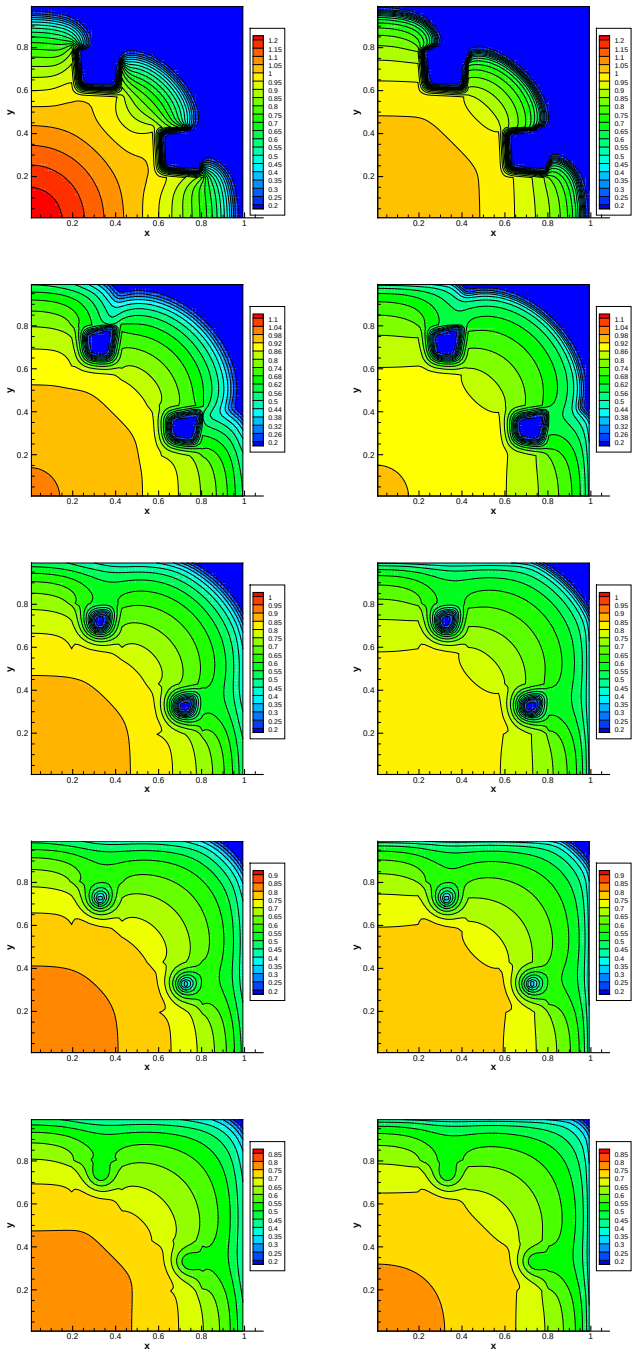


Figure 5: Hard problem (Example 6.1) with parameter $\epsilon = 10^{-2}$ for material temperature on the left, and radiation temperature on the right. At five output times $t = 0.6, 1.2, 1.8, 2.4$, and 3.0, from top to bottom. In Comparison with the strong scattering results in Fig. 4, the free transport phenomena is observed in this case.

https://doi.org/10.4208/cicp.OA-2016-0261 Published online by Cambridge University Press

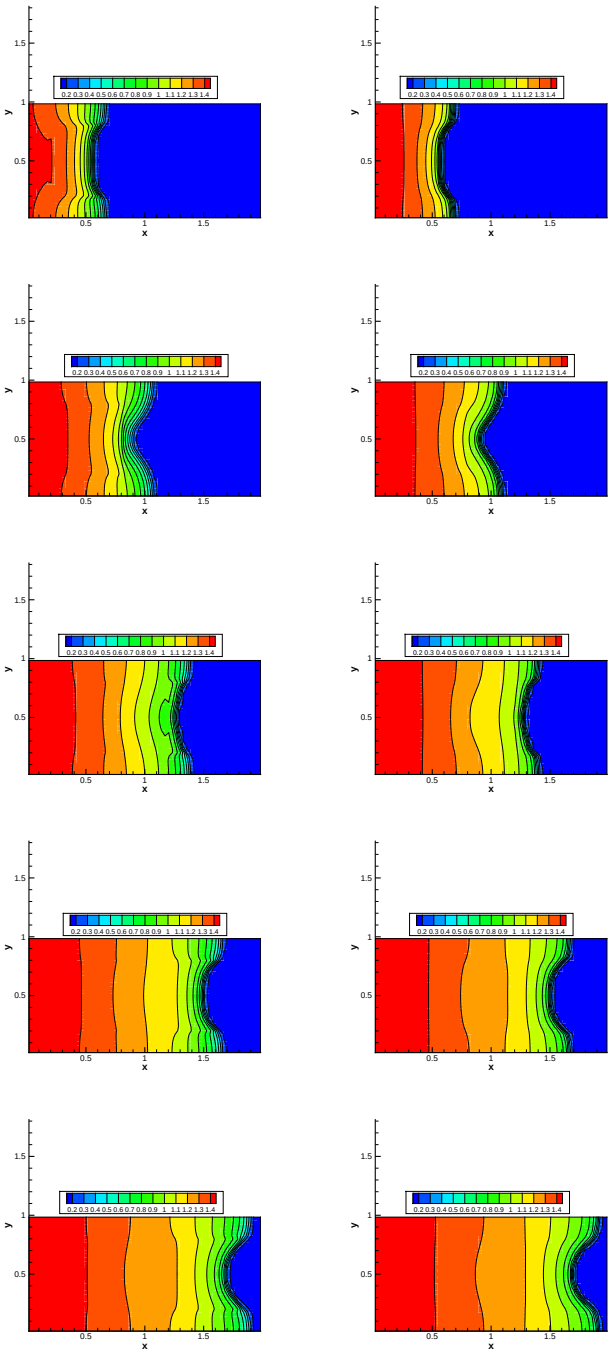


Figure 6: Easy problem (Example 6.2) with parameter $\epsilon = 10^{-6}$ for material temperature on the left, and radiation temperature on the right. At five output times $t = 0.6, 1.2, 1.8, 2.4$, and 3.0 from top to bottom. Different material and radiation temperature can be identified in the evolution process.

https://doi.org/10.4208/cicp.OA-2016-0261 Published online by Cambridge University Press

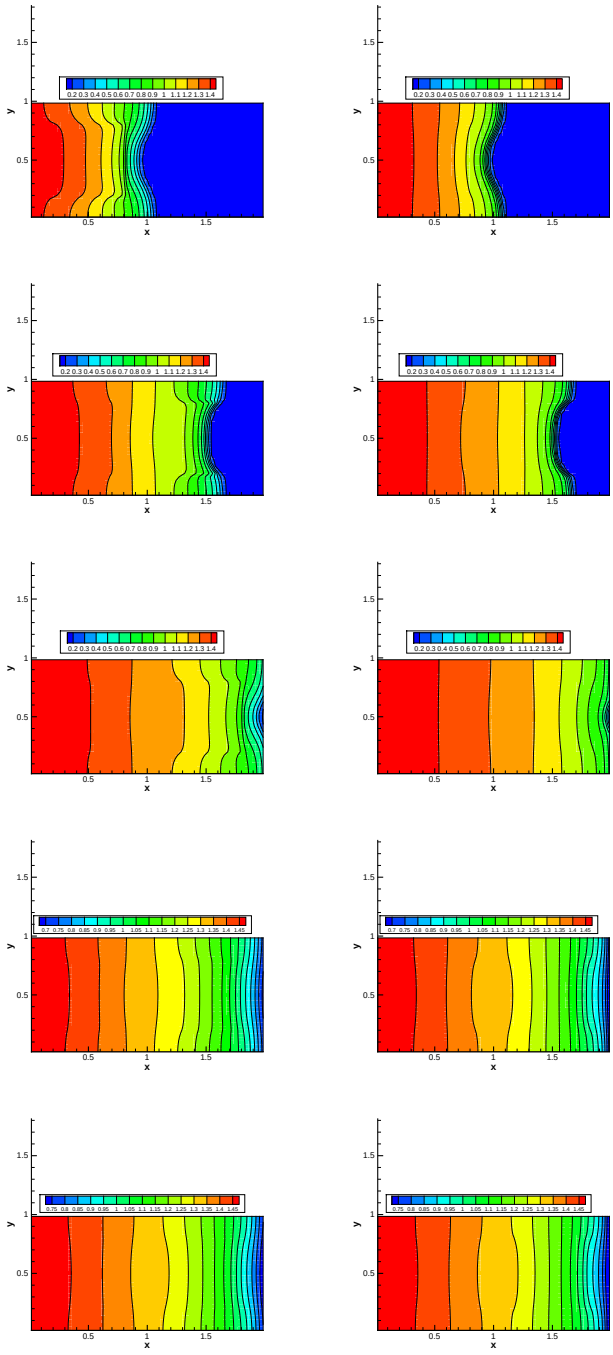


Figure 7: Easy problem (Example 6.2) with parameter $\epsilon = 10^{-2}$ for material temperature on the left, and radiation temperature on the right. At five output times $t = 0.6, 1.2, 1.8, 2.4$, and 3.0 from top to bottom. In comparison with the results of strong scattering case in Fig. 6, the free transport phenomena is observed in this case.

https://doi.org/10.4208/cicp.OA-2016-0261 Published online by Cambridge University Press

and scattering two asymptotic limits, equilibrium and non-equilibrium, can be accurately recovered. For the strong absorption/emission case, an equilibrium diffusive limit is obtained, where the system is driven by the material temperature with a nonlinear diffusion equation. However, for the strong scattering case, the non-equilibrium diffusive limit, with nonlinearly coupled radiation temperature and material temperature governing equations, is recovered. Besides recovering the equilibrium and non-equilibrium diffusive limits, the IUGKS can present reliable and accurate solutions in the whole transition regime as well, from optical thin and optical thick regions smoothly. With the variation of the ratio between the mesh size and the photon's mean free path, a continuum radiative transport mechanism is modeled and evolved in the UGKS method. The numerical examples validate the current approach. In the future, the method will be further extended to couple the radiative transfer with the hydrodynamic equations.

Acknowledgments

The authors would like to thank all referees for their constructive comments and suggestions for the improvement of the paper. The current research of Sun is supported by NSFC (Grant Nos. 11671048, 91630310, 11371068) and the Science and Technology Development foundation of China Academy of Engineering Physics (Grant Nos. 2015B0202041, 2015B0202040); and Jiang is supported by the National Basic Research Program under Grant 2014CB745002 and NSFC (Grant Nos. 11229101, 11631008, 11371065); The research work of Xu is supported by Hong Kong research grant council (16207715, 16211014, 620813) and NSFC (91330203, 91530319).

References

[1] S.Z. Chen, K. Xu, C.B. Lee, and Q.D. Cai, *A unified gas kinetic scheme with moving mesh and velocity space adaptation*, J. Comput. Phys. **231** (2012), pp. 6643-6664.
[2] N.A. Gentile, *Implicit Monte Carlo diffusion - an accerlation method for Monte Carlo time-dependent radiative transfer simulations.* J. Comput. Phys., **172** (2001), 543-571.
[3] J.C. Huang, K. Xu, and P.B. Yu, *A unified gas-kinetic scheme for continuum and rarefied flows II: multi-dimensional cases*, Communications in Computational Physics, **12**, no. 3 (2012), pp. 662-690.
[4] S. Jin and C.D. Levermore, *The discrete-ordinate method in diffusive regimes,* Transport Theory Statist. Phys., **20(5-6)**, (1991), 413-439.
[5] S. Jin, L. Pareschi and G. Toscani, *Uniformly accurate diffusive relaxation schemes for multiscale transport equations,* SIAM J. Numer. Anal., **38(3)** (2000), 913-936.
[6] A. Klar, *An asymptotic-induced scheme for nonstationary transport equations in the diffusive limit,* SIAM J. Numer. Anal., **35(6)** (1998), 1073-1094.
[7] A.W. Larsen and J.E. Morel, *Asymptotic solutions of numerical transport problems in optically thick, diffusive regimes. II,* J. Comp. Phys., **83(1)** (1989), 212-236.
[8] A.W. Larsen, J.E. Morel and W.F. Miller Jr., *Asymptotic solutions of numerical transport problems in optically thick, diffusiive regimes.* J. Comput. Phys., **69(2)** (1987), 283-324.

https://doi.org/10.4208/cicp.OA-2016-0261 Published online by Cambridge University Press

[9] C.E. Lee, *The Discrete S_N Approximation to Transport Theory,* LA-2595, 1962.
[10] L. Mieussens, *On the asymptotic preserving property of the unified gas kinetic scheme for the diffusion limit of linear kinetic model.* J. Comput. Phys. **253** (2013), 138-156.
[11] B. van Leer, *Towards the ultimate conservative difference schemes V. A second-order sequal to Godunov's method*. J. Comput. Phys. **32** (1979), 101-136.
[12] K. Xu and J.C. Huang, *A unified gas-kinetic scheme for continuum and rarefied flows.* J. Comput. Phys., **229** (2010), 7747-7764.
[13] L. Spitzer and R. Harm, *Transport phenomena in a completely ionized gas.* Phys. Rev., **89** (1953), 977.
[14] W.J. Sun, S. Jiang, and K. Xu, *An Asymptotic Preserving unified gas kinetic scheme for gray radiative transfer equations.* J. Comput. Phys. **285** (2015), pp. 265-279.
[15] W.J. Sun, S. Jiang, K. Xu and S. Li, *An Asymptotic Preserving unified gas kinetic scheme for frequency-dependent radiative transfer equations.* J. Comput. Phys. **302** (2015), pp. 222-238.
[16] V.A. Mousseau and D.A. Knoll, *Temporal accuracy of the nonequilibrium radiation diffusion equations applied to two-dimensional multimaterial simulations.* Nuclear Science and Engineering, **154** (2006), pp. 174-189.
[17] B. Chang, *The incorporation of the semi-implicit linear equations into Newton's method to solve radiation transfer equations.* J. Comput. Phys., **226** (2007), pp. 852-878.
[18] E.W. Larsen, *A grey transport acceleration method for time-dependent radiative transfer problems.* J. Comput. Phys. **78** (1988), pp. 459-480.
[19] P. Godillon-Lafitte And T. Goudon, *A Coupled Model For Radiative Transfer: Doppler Effects, Equilibrium, And Nonequilibrium Diffusion Asymptotics.* Multiscale Model. Simul., **4(4)** (2005), pp. 1245C1279.
[20] C. Bueta and B. Despresa, *Asymptotic analysis of (uid models for the coupling of radiation and hydrodynamics.* Journal of Quantitative Spectroscopy and Radiative Transfer **85** (2004), PP. 385C418.

https://doi.org/10.4208/cicp.OA-2016-0261 Published online by Cambridge University Press